ELSEVIER
Available online at www.sciencedirect.com
ScienceDirect
Journal of Computational and Applied Mathematics 218 (2008) 34–42
JOURNAL OF COMPUTATIONAL AND APPLIED MATHEMATICS
www.elsevier.com/locate/cam

Numerical simulation of airfoil vibrations induced by turbulent flow☆

Lenka Dubcová[a,*], Miloslav Feistauer[a], Jaroslav Horáček[b], Petr Sváček[c]

[a] *Faculty of Mathematics and Physics, Charles University Prague, Sokolovská 83, 186 75 Praha 8, Czech Republic*
[b] *Institute of Thermomechanics, Academy of Sciences of the Czech Republic, Dolejškova 5, 182 00 Praha 8, Czech Republic*
[c] *Faculty of Mechanical Engineering, Czech Technical University in Prague, Karlovo nám. 13, 121 35 Praha 2, Czech Republic*

Received 25 January 2007

Abstract

The subject of this paper is the numerical simulation of the interaction between two-dimensional incompressible viscous flow and a vibrating airfoil. A solid elastically supported airfoil with two degrees of freedom, which can rotate around the elastic axis and oscillate in the vertical direction, is considered. The numerical simulation consists of the stabilized finite element solution of the Reynolds averaged Navier–Stokes equations with algebraic models of turbulence, coupled with the system of ordinary differential equations describing the airfoil motion. Since the computational domain is time dependent and the grid is moving, the Arbitrary Lagrangian–Eulerian (ALE) method is used. The developed method was applied to the simulation of flow-induced airfoil vibrations.

MSC: 74S05; 76D05

Keywords: Aeroelasticity; Stabilized finite element method; ALE formulation; Algebraic turbulent models; Flow-induced airfoil vibrations; Flutter

1. Introduction

The interaction between fluid flow and elastic structures plays an important role in many technical disciplines—airplane industry (e.g., wings vibrations), blade machines (oscillations of blades in turbines and compressors), civil engineering (interaction of a strong wind with TV towers, cooling towers or bridges), etc. The research in aeroelasticity or hydroelasticity focuses on the interaction between flowing fluids and vibrating structures (see, e.g., [5] and [10]).

In [15], the problem of the flow-induced airfoil vibrations is analyzed with the aid of the finite element method. The finite element solution of the Navier–Stokes equations written in the arbitrary Lagrangian–Eulerian (ALE) form is coupled with the numerical solution of the system of ordinary differential equations describing the airfoil motion.

Since the Reynolds number is rather high (10^5–10^7), it is necessary to take into account the effects caused by turbulence. The present paper represents an extension of the methods and results obtained in [15] by including a model

☆ This research was supported by the Grant no. 201/05/0005 of the Grant Agency of the Czech Republic and the Grant no. IAA200760613 of the Grant Agency of the Academy of Sciences of the Czech Republic. This research was also partly supported by the Research Projects MSM 0021620839 (M. Feistauer) and 6840770003 (P. Sváček) of the Ministry of Education of the Czech Republic.
* Corresponding author.
E-mail addresses: ldubcova@utep.edu (L. Dubcová), feist@karlin.mff.cuni.cz (M. Feistauer).

0377-0427/$ - see front matter
doi:10.1016/j.cam.2007.04.042

of turbulence in the simulation process. We apply and test here the algebraic models of turbulence designed by Baldwin and Lomax [1] and by Rostand [12]. As a result we obtain a sufficiently accurate and robust method, which we apply to the simulation of flow-induced airfoil vibrations.

2. Continuous problem

We assume that $(0, T)$ is a time interval and by $\Omega_t \subset \mathbb{R}^2$ we denote a bounded computational domain occupied by the fluid at time t. The symbols $\boldsymbol{u} = \boldsymbol{u}(x, t)$ and $p = p(x, t)$, $x \in \Omega_t$, $t \in (0, T)$, denote the flow velocity and the kinematic pressure (i.e., dynamic pressure divided by the density ρ of the fluid) and v denotes the kinematic viscosity. We have $\boldsymbol{u} = (u_1, u_2)$, where u_1 and u_2 are the components of the velocity in the directions of the Cartesian coordinates x_1 and x_2 of x.

The character of the flow depends on the magnitude of the Reynolds number $Re = Uc/v$, where U denotes the characteristic velocity (in our case the magnitude of the far field velocity) and c is the characteristic length (here the length of the airfoil chord). The flow with a sufficiently small Reynolds number is laminar. If the Reynolds number is larger than some critical value, the flow becomes turbulent.

We use the models of turbulence based on the so-called Reynolds averaged equations and the Boussinesq hypothesis [8,13], which yield the Reynolds averaged equations in the form

$$\nabla \cdot \boldsymbol{u} = 0,$$
$$\frac{\partial u_i}{\partial t} + (\boldsymbol{u} \cdot \nabla) u_i + \frac{\partial p}{\partial x_i} - \sum_{j=1}^{2} \frac{\partial}{\partial x_j} \left\{ (v + v_{\mathrm{T}}) \left(\frac{\partial u_i}{\partial x_j} + \frac{\partial u_j}{\partial x_i} \right) \right\} = 0, \quad i = 1, 2. \tag{2.1}$$

Here v_{T} is the so-called turbulent viscosity. It is computed on the basis of various turbulence models.

System (2.1) is equipped with the initial condition

$$\boldsymbol{u}(x, 0) = \boldsymbol{u}_0, \quad x \in \Omega_0, \tag{2.2}$$

and boundary conditions

$$\text{(a) } \boldsymbol{u}|_{\Gamma_D} = \boldsymbol{u}_D, \quad \text{(b) } \boldsymbol{u}|_{\Gamma_{Wt}} = \boldsymbol{w}|_{\Gamma_{Wt}},$$
$$\text{(c) } -(p - p_{\mathrm{ref}}) n_i + (v + v_{\mathrm{T}}) \sum_{j=1}^{2} \left(\frac{\partial u_i}{\partial x_j} + \frac{\partial u_j}{\partial x_i} \right) n_j = 0 \quad \text{on } \Gamma_{\mathrm{O}}, \quad i = 1, 2. \tag{2.3}$$

Here $\boldsymbol{n} = (n_1, n_2)$ is the unit outer normal to the boundary $\partial\Omega_t$ of the domain Ω_t, Γ_{D} represents the inlet (and, possibly, fixed impermeable walls), Γ_{O} is the outlet and Γ_{Wt} is the boundary of the airfoil at time t. Condition (2.3), (b) represents the assumption that the fluid adheres to the airfoil moving with the velocity $\boldsymbol{w}|_{\Gamma_{Wt}}$. By p_{ref} we denote a prescribed reference (far field) pressure.

The vertical displacement H of the elastic axis $x_{\mathrm{EO}} = (x_{\mathrm{EO1}}, x_{\mathrm{EO2}})$ (oriented downwards) and the rotation α of the airfoil around the elastic axis (oriented clockwise) are described by the system [15]

$$m\ddot{H} + S_\alpha \ddot{\alpha} \cos\alpha + k_{HH} H + d_{HH} \dot{H} - S_\alpha \dot{\alpha}^2 \sin\alpha = -L(t),$$
$$S_\alpha \ddot{H} \cos\alpha + I_\alpha \ddot{\alpha} + k_{\alpha\alpha} \alpha + d_{\alpha\alpha} \dot{\alpha} = M(t), \tag{2.4}$$

where m denotes the mass of the airfoil, S_α, I_α are the static moment and the inertia moment around the elastic axis, k_{HH}, $k_{\alpha\alpha}$ denote the bending stiffness and the torsional stiffness, d_{HH}, $d_{\alpha\alpha}$ are the structural dampings. The aerodynamic lift force $L(t)$ and the aerodynamic torsional moment $M(t)$ are defined by the relations

$$L = -\ell \int_{\Gamma_{Wt}} \sum_{j=1}^{2} \tau_{2j} n_j \,\mathrm{d}S, \quad M = \ell \int_{\Gamma_{Wt}} \sum_{i,j=1}^{2} \tau_{ij} n_j r_i^{\mathrm{ort}} \,\mathrm{d}S,$$
$$\tau_{ij} = \rho \left[-p\delta_{ij} + v \left(\frac{\partial u_i}{\partial x_j} + \frac{\partial u_j}{\partial x_i} \right) \right], \quad r_1^{\mathrm{ort}} = -(x_2 - x_{\mathrm{EO2}}), \quad r_2^{\mathrm{ort}} = x_1 - x_{\mathrm{EO1}}. \tag{2.5}$$

The symbol ℓ denotes the depth of the airfoil. These relations determine the interaction between the moving fluid and the airfoil.

3. Discrete problem

3.1. ALE method

In order to simulate flow in a moving domain, we employ the ALE method (cf. [11]), based on a one-to-one ALE mapping

$$\mathscr{A}_t : \Omega_{\mathrm{ref}} \to \Omega_t, \quad X \mapsto x(X,t) = \mathscr{A}_t(X) \tag{3.1}$$

of the reference configuration $\Omega_{\mathrm{ref}} = \Omega_0$ onto the current configuration Ω_t, with the domain velocity $\boldsymbol{w} = \partial \mathscr{A}_t / \partial t$. We suppose that the domain velocity at each point on the surface of the airfoil is equal to the velocity of its motion. By $\mathrm{D}^{\mathscr{A}}/\mathrm{D}t$ we denote the ALE derivative—i.e., derivative with respect to the reference configuration. This means that for a function $f : \{(x,t); x \in \Omega_t, t \in [0,T]\} \to \mathbb{R}$ and $x = \mathscr{A}_t(X), X \in \Omega_{\mathrm{ref}}$, we introduce the function $\tilde{f}(X,t) = f(\mathscr{A}_t(X), t)$ and define

$$\frac{\mathrm{D}^{\mathscr{A}} f}{\mathrm{D}t}(x,t) = \frac{\partial \tilde{f}}{\partial t}(X,t). \tag{3.2}$$

With the aid of the ALE method we rewrite system (2.1) in the form (see [14])

$$\begin{aligned} &\nabla \cdot \boldsymbol{u} = 0, \\ &\frac{\mathrm{D}^{\mathscr{A}}}{\mathrm{D}t} u_i + ((\boldsymbol{u} - \boldsymbol{w}) \cdot \nabla) u_i + \frac{\partial p}{\partial x_i} - \sum_{j=1}^{2} \frac{\partial}{\partial x_j} \left\{ (\nu + \nu_{\mathrm{T}}) \left(\frac{\partial u_i}{\partial x_j} + \frac{\partial u_j}{\partial x_i} \right) \right\} = 0, \quad i = 1, 2. \end{aligned} \tag{3.3}$$

3.2. Time discretization

We consider a partition $0 = t_0 < t_1 < \cdots < T$, $t_{\mathrm{k}} = k\tau$ of the time interval $[0,T]$ with a time step $\tau > 0$ and use the approximations $\boldsymbol{u}(t_n) \approx \boldsymbol{u}^n$ and $p(t_n) \approx p^n$ of the exact solution and $\boldsymbol{w}(t_n) \approx \boldsymbol{w}^n$ of the domain velocity at time t_n. Using the second-order backward difference formula for the approximation of the ALE derivative and setting $\hat{\boldsymbol{u}}^k = \boldsymbol{u}^k \circ \mathscr{A}_{t_{\mathrm{k}}} \circ \mathscr{A}_{t_{n+1}}^{-1}$ (which is defined in $\Omega_{t_{n+1}}$), we obtain the system

$$\nabla \cdot \boldsymbol{u}^{n+1} = 0, \tag{3.4}$$

$$\begin{aligned} &\frac{3u_i^{n+1} - 4\hat{u}_i^n + \hat{u}_i^{n-1}}{2\tau} + ((\boldsymbol{u}^{n+1} - \boldsymbol{w}^{n+1}) \cdot \nabla) u_i^{n+1} + \frac{\partial p^{n+1}}{\partial x_i} \\ &\quad - \sum_{j=1}^{2} \frac{\partial}{\partial x_j} \left\{ (\nu + \nu_T(\boldsymbol{u}^{n+1})) \left(\frac{\partial u_i^{n+1}}{\partial x_j} + \frac{\partial u_j^{n+1}}{\partial x_i} \right) \right\} = 0, \quad i = 1, 2 \quad \text{in } \Omega_{t_{n+1}}. \end{aligned} \tag{3.5}$$

3.3. Finite element space discretization

The starting point for the space discretization by the finite element method is the weak formulation. For simplicity we set $\Omega = \Omega_{t_{n+1}}$, $\boldsymbol{u} = \boldsymbol{u}^{n+1}$, $p = p^{n+1}$. We define the function spaces $W = (H^1(\Omega))^2$, $X = \{\boldsymbol{v} \in W; \boldsymbol{v}|_{\Gamma_D \cup \Gamma_{W_t}} = 0\}$, $Q = L^2(\Omega)$, where $L^2(\Omega)$ is the Lebesgue space of square integrable functions over the domain Ω and $H^1(\Omega) = \{v \in L^2(\Omega); \partial v / \partial x_i \in L^2(\Omega), i = 1, 2\}$ is the Sobolev space. By $(\cdot, \cdot)_\Omega$ we denote the $L^2(\Omega)$-scalar product.

The weak formulation is obtained in a standard way. Eq. (3.4) is multiplied by a test function $q \in Q$, and Eq. (3.5) is multiplied by a test function $\boldsymbol{v} \in X$, integrated over the domain Ω, Green's theorem is applied, the boundary condition (2.3), (c) is used and the resulting integral identities are summed. Under the notation $\boldsymbol{U} = (\boldsymbol{u}, p)$, $\boldsymbol{U}^* = (\boldsymbol{u}^*, p)$, $\boldsymbol{V} = (\boldsymbol{v}, q)$

and

$$a(\boldsymbol{U}^*, \boldsymbol{U}, \boldsymbol{V}) = \frac{3}{2\tau}(\boldsymbol{u}, \boldsymbol{v})_\Omega + (((\boldsymbol{u}^* - \boldsymbol{w}^{n+1}) \cdot \nabla)\boldsymbol{u}, \boldsymbol{v})_\Omega - (p, \operatorname{div} \boldsymbol{v})_\Omega + \sum_{i,j=1}^{2} \int_\Omega \frac{1}{2}(\nu + \nu_{\mathrm{T}}) \left(\frac{\partial u_i}{\partial x_j} + \frac{\partial u_j}{\partial x_i}\right)\left(\frac{\partial v_i}{\partial x_j} + \frac{\partial v_j}{\partial x_i}\right) \mathrm{d}x + (\operatorname{div} \boldsymbol{u}, q)_\Omega, \tag{3.6}$$

$$f(\boldsymbol{V}) = \frac{1}{2\tau}(4\hat{\boldsymbol{u}}^n - \hat{\boldsymbol{u}}^{n-1}, \boldsymbol{v})_\Omega - \int_{\Gamma_O} p_{\mathrm{ref}} \boldsymbol{n} \cdot \boldsymbol{v} \, \mathrm{d}S, \tag{3.7}$$

we define a weak solution as a couple $\boldsymbol{U} = (\boldsymbol{u}, p) \in W \times Q$ such that $\boldsymbol{u}$ satisfies the boundary conditions (2.3), (a)–(b), and

$$a(\boldsymbol{U}, \boldsymbol{U}, \boldsymbol{V}) = f(\boldsymbol{V}) \quad \forall \boldsymbol{V} = (\boldsymbol{v}, q) \in X \times Q. \tag{3.8}$$

On the basis of the weak formulation we introduce a finite element solution. We approximate the spaces W, X, Q by subspaces W_h, X_h, Q_h, $h \in (0, h_0)$, $h_0 > 0$, where $X_h = W_h \cap X$. The approximate solution is defined as a couple $\boldsymbol{U}_h = (\boldsymbol{u}_h, p_h) \in W_h \times Q_h$ such that

$$a(\boldsymbol{U}_h, \boldsymbol{U}_h, \boldsymbol{V}_h) = f(\boldsymbol{V}_h), \quad \forall \boldsymbol{V}_h = (\boldsymbol{v}_h, q_h) \in X_h \times Q_h \tag{3.9}$$

and $\boldsymbol{u}_h$ satisfies an approximation of the boundary conditions (2.3), (a)–(b).

The finite element spaces are constructed in the following way. Let Ω be a polygonal domain and $\mathscr{T}_h$ its triangulation formed by a finite number of closed triangles with standard properties from the finite element method. We use the well-known Taylor–Hood P_2/P_1 elements:

$$p \approx p_h \in Q_h = \{q \in Q \cap C(\bar{\Omega});\, q|_K \in P_1(K), \forall K \in \mathscr{T}_h\} \tag{3.10}$$

and

$$\boldsymbol{u} \approx \boldsymbol{u}_h \in W_h = \{\boldsymbol{v} \in W \cap (C(\bar{\Omega}))^2;\, \boldsymbol{v}|_K \in (P_2(K))^2, \forall K \in \mathscr{T}_h\}, \quad X_h = W_h \cap X. \tag{3.11}$$

Here $P_k(K)$ denotes the space of all polynomials on $K \in \mathscr{T}_h$ of degree $\leqslant k$. The spaces X_h, Q_h satisfy the Babuška–Brezzi condition (cf. [7]).

3.4. Stabilized finite element method

For large Reynolds numbers our problem becomes singularly perturbed with dominating convection, and approximate solutions can contain nonphysical spurious oscillations. In order to avoid them, we apply the stabilization by the streamline–diffusion method combined with the pressure stabilization. We set $\overline{\boldsymbol{w}} = \boldsymbol{u}^* - \boldsymbol{w}^{n+1}$ and for $\boldsymbol{U} = (\boldsymbol{u}, p)$, $\boldsymbol{U}^* = (\boldsymbol{u}^*, p)$, $\boldsymbol{V} = (\boldsymbol{v}, q)$, $\boldsymbol{D}(\boldsymbol{u}) = ((\partial u_i/\partial x_j + \partial u_j/\partial x_i)/2))_{i,j=1}^2$, introduce the stabilization forms

$$\mathscr{L}_h(\boldsymbol{U}^*, \boldsymbol{U}, \boldsymbol{V}) = \sum_{K \in \mathscr{T}_h} \delta_K \left(\frac{3}{2\tau}\boldsymbol{u} - \nabla \cdot \{2(\nu + \nu_T)\boldsymbol{D}(\boldsymbol{u})\} + (\overline{\boldsymbol{w}} \cdot \nabla)\boldsymbol{u} + \nabla p, (\overline{\boldsymbol{w}} \cdot \nabla)\boldsymbol{v}\right)_K, \tag{3.12}$$

$$\mathscr{F}_h(\boldsymbol{V}) = \sum_{K \in \mathscr{T}_h} \delta_K \left(\frac{1}{2\tau}(4\hat{\boldsymbol{u}}^n - \hat{\boldsymbol{u}}^{n-1}), (\overline{\boldsymbol{w}} \cdot \nabla)\boldsymbol{v}\right)_K, \tag{3.13}$$

and

$$\mathscr{P}_h(\boldsymbol{U}, \boldsymbol{V}) = \sum_{K \in \mathscr{T}_h} \tau_K (\nabla \cdot \boldsymbol{u}, \nabla \cdot \boldsymbol{v})_K. \tag{3.14}$$

The symbol $(\cdot, \cdot)_K$ denotes the scalar product in the space $L^2(K)$ and $\delta_K \geqslant 0$ and $\tau_K \geqslant 0$ are suitable parameters.

The stabilized discrete problem is formulated in the following way. Find $\boldsymbol{U}_h = (\boldsymbol{u}_h, p_h) \in W_h \times Q_h$ such that $\boldsymbol{u}_h$ satisfies an approximation of the boundary conditions (2.3), (a)–(b) and

$$a(\boldsymbol{U}_h, \boldsymbol{U}_h, \boldsymbol{V}_h) + \mathscr{L}_h(\boldsymbol{U}_h, \boldsymbol{U}_h, \boldsymbol{V}_h) + \mathscr{P}_h(\boldsymbol{U}_h, \boldsymbol{V}_h) = f(\boldsymbol{V}_h) + \mathscr{F}_h(\boldsymbol{V}_h)$$
$$\text{for all } \boldsymbol{V}_h = (\boldsymbol{v}_h, q_h) \in X_h \times Q_h. \tag{3.15}$$

Parameters δ_K and τ_K are chosen according to [6,9].

The discrete stabilized nonlinear problem (3.15) at time $t = t_{n+1}$ is solved with the aid of the Oseen iterations

$$a(\boldsymbol{U}_h^{(\ell)}, \boldsymbol{U}_h^{(\ell+1)}, \boldsymbol{V}_h) + \mathscr{L}_h(\boldsymbol{U}_h^{(\ell)}, \boldsymbol{U}_h^{(\ell+1)}, \boldsymbol{V}_h) + \mathscr{P}_h(\boldsymbol{U}_h^{(\ell+1)}, \boldsymbol{V}_h)$$
$$= f(\boldsymbol{V}_h) + \mathscr{F}_h(\boldsymbol{V}_h) \quad \text{for all } \boldsymbol{V}_h = (\boldsymbol{v}_h, q_h) \in X_h \times Q_h, \quad \ell = 0, 1, \ldots. \tag{3.16}$$

The initial approximation $\boldsymbol{U}_h^{(0)}$ is defined on the basis of the approximate solution on the previous time level t_n. Problem (3.16) is equivalent to a system of linear algebraic equations, which is solved by the direct solver UMFPACK [3], which is efficient up to 10^5 unknowns. For larger problems suitable iterative method should be used.

The computation of the force L and the moment M at time $t = t_{n+1}$ from the approximate solution is carried out with aid of a weak reformulation similarly as in [14].

4. Algebraic models of turbulence

Now it remains to specify the evaluation of the turbulent viscosity ν_{T}. For this purpose we use algebraic models of turbulence.

4.1. Cebeci–Smith (CS) model

A basis for the application of algebraic models of turbulence is the Cebeci–Smith (CS) model [2]. In this model, the computational domain Ω is divided into an inner domain near the wall (airfoil), where the internal turbulent viscosity ν_{Ti} is evaluated. In the outer part of the computational domain, the outer turbulence viscosity ν_{To} is computed. In practical computations, both the viscosities are evaluated in the whole domain Ω and then the turbulent viscosity is defined as

$$\nu_{\mathrm{T}} = \min(\nu_{\mathrm{Ti}}, \nu_{\mathrm{To}}). \tag{4.1}$$

The turbulent viscosity is computed with the aid of a local coordinate system (X, Y), where X is measured along the airfoil or along the axis of the wake and the axis Y is orthogonal to X. Components of the velocity in the directions X and Y are denoted by U and V (Fig. 1). The inner turbulent viscosity is defined by

$$\nu_{\mathrm{Ti}} = \rho l^2 \left| \frac{\partial U}{\partial Y} \right|, \tag{4.2}$$

where ρ is the fluid density and l is the mixing length, which is determined by the relations

$$l = \kappa Y F_{\mathrm{D}}, \quad F_{\mathrm{D}} = 1 - \exp\left(-\frac{1}{A^+} \frac{u_\tau Y}{\nu} \right). \tag{4.3}$$

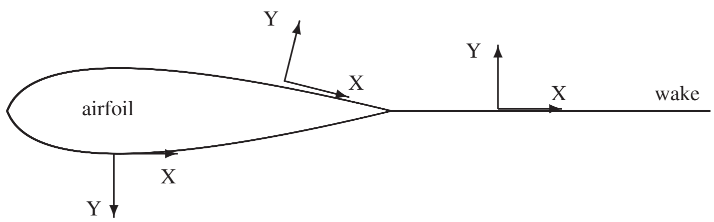

Fig. 1. Local coordinates X, Y.

F_D is the so-called van Driest function. The symbol $Y = Y(x)$ denotes the orthogonal distance of a point $x \in \Omega$ from the airfoil or the axis of the wake. The so-called shear velocity u_τ is defined by

$$u_\tau = \left(v \left| \frac{\partial U}{\partial Y} \right| \right)_w^{1/2}. \tag{4.4}$$

The subscript w means the value for $Y=0$. The empirical constant $A^+=26$ was determined for $\kappa=0.4$ from experimental data obtained from the flow around a plate. In the wake we set $v_{\mathrm{Ti}} = \infty$.

The outer turbulent viscosity is defined by the Clauser relation

$$v_{\mathrm{To}} = \rho \alpha \delta_i^* U_e F_{\mathrm{k}}, \tag{4.5}$$

where $\alpha = 0.0168$,

$$F_{\mathrm{k}} = \left[1 + 5.5 \left(\frac{Y}{\delta} \right)^6 \right]^{-1}, \tag{4.6}$$

δ is the shear layer thickness, $U_e = U(\delta)$ represents the velocity of the outer flow and δ_i^* is the kinematic displacement thickness

$$\delta_i^* = \int_0^\delta \left(1 - \frac{U}{U_e} \right) \mathrm{d}Y. \tag{4.7}$$

The given algebraic model requires to know the quantities δ, $U_e \delta_i^*$ and u_τ, which is not suitable for the solution of our problem. Therefore, in the sequel we consider some modifications of the CS model.

4.2. Baldwin–Lomax (BL) model

Baldwin and Lomax [1] proposed the following modification of the CS model. The inner turbulent viscosity is defined as

$$v_{\mathrm{Ti}} = \rho l^2 |\omega|, \tag{4.8}$$

where

$$\omega = \frac{\partial U}{\partial Y} - \frac{\partial V}{\partial X} \tag{4.9}$$

is the vorticity. The outer turbulent viscosity is determined by the relations

$$v_{\mathrm{To}} = \rho \alpha C_{\mathrm{cp}} F_w F_{\mathrm{k}}, \tag{4.10}$$

$$F_w = \min(F_{w_1}, F_{w_2}), \quad F_{w_1} = Y_{\max} F_{\max}, \quad F_{w_2} = C_{wk}\, Y_{\max} \frac{(\Delta U)^2}{F_{\max}}. \tag{4.11}$$

The value $F_{\max}$ is the maximum of the function $F = Y|\omega| F_D$ on the line $X = \text{const.}$, $Y \geqslant 0$, $Y_{\max}$ is the value, for which $F(Y_{\max}) = F_{\max}$ and ΔU is the maximum variation of the velocity U along the line $X = \text{const.}$, $Y \geqslant 0$. For the Klebanoff function F_{k} we have

$$F_{\mathrm{k}} = \left[1 + 5.5 \left(C_{\mathrm{KL}} \frac{Y}{Y_{\max}} \right)^6 \right]^{-1}. \tag{4.12}$$

Further, the shear layer thickness δ is expressed as $\delta = Y_{\max}/C_{\mathrm{KL}}$. Baldwin and Lomax use the following constants $\alpha = 0.0168,\ C_{\mathrm{cp}} = 1.6,\ C_{\mathrm{KL}} = 0.3,\ C_{\mathrm{wk}} = 0.25$.

We also applied the Rostand model [12], which gives comparable results.

5. Flow-induced airfoil vibrations

This section presents results of the numerical simulation of flow-induced vibrations obtained for the airfoil NACA 0012. The following quantities, used in [15], are considered: $m = 0.086622\,\mathrm{kg}$, $S_\alpha = -0.000779673\,\mathrm{kg\,m}$, $I_\alpha = 0.000487291\,\mathrm{kg\,m^2}$, $k_{HH} = 105.109\,\mathrm{N/m}$, $k_{\alpha\alpha} = 3.695582\,\mathrm{N\,m/rad}$, $\ell = 0.05\,\mathrm{m}$, $c = 0.3\,\mathrm{m}$, $\rho = 1.225\,\mathrm{kg/m^3}$, $v = 1.5 \cdot 10^{-5}\,\mathrm{m/s^2}$. The positions of the elastic axis and the center of gravity of the airfoil measured along the chord from the leading edge are $x_{\mathrm{EO1}} = 0.4c = 0.12\,\mathrm{m}$, and $x_{T1} = 0.37c = 0.111\,\mathrm{m}$, respectively. The coefficients of the proportional damping are considered in the form $d_{HH} = \varepsilon k_{HH}$ and $d_{\alpha\alpha} = \varepsilon k_{\alpha\alpha}$, where we choose $\varepsilon = 10^{-3}$.

The computational process for the solution of the nonstationary problem is based on the coupling of the fluid flow problem in the discrete form (3.15) with the numerical solution of the nonlinear structural model (2.4) by the fourth order Runge–Kutta method. It starts at time $t = 0$ by the solution of the flow, keeping the airfoil in a fixed position given by the prescribed initial translation $H_0 = 10\,\mathrm{mm}$ and the angle of attack $\alpha_0 = -7°$. Then, at time $\delta t > 0$ the airfoil is released and we continue by the solution of a complete fluid–structure interaction problem with $H(\delta t) = H_0$, $\dot{H}(\delta t) = 0$, $\alpha(\delta t) = \alpha_0$, $\dot{\alpha}(\delta t) = 0$. The computational mesh was constructed in an adaptive way with the aid of the package ANGENER [4].

The simulation of the airfoil motion due to the fluid–structure interaction in time domain is shown in Figs. 2–4 for the far field velocity $U_\infty = 30$, 35 and 40 m/s. The corresponding Reynolds number has the values $Re = 6 \cdot 10^5$, $7 \cdot 10^5$ and $8 \cdot 10^5$.

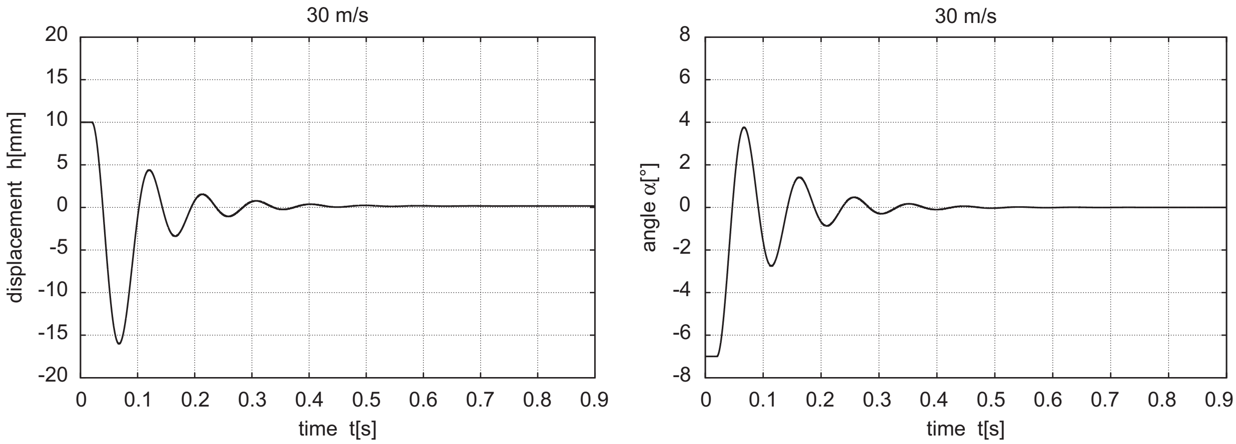

Fig. 2. Flow-induced airfoil vibrations for $U_\infty = 30\,\mathrm{m/s}$.

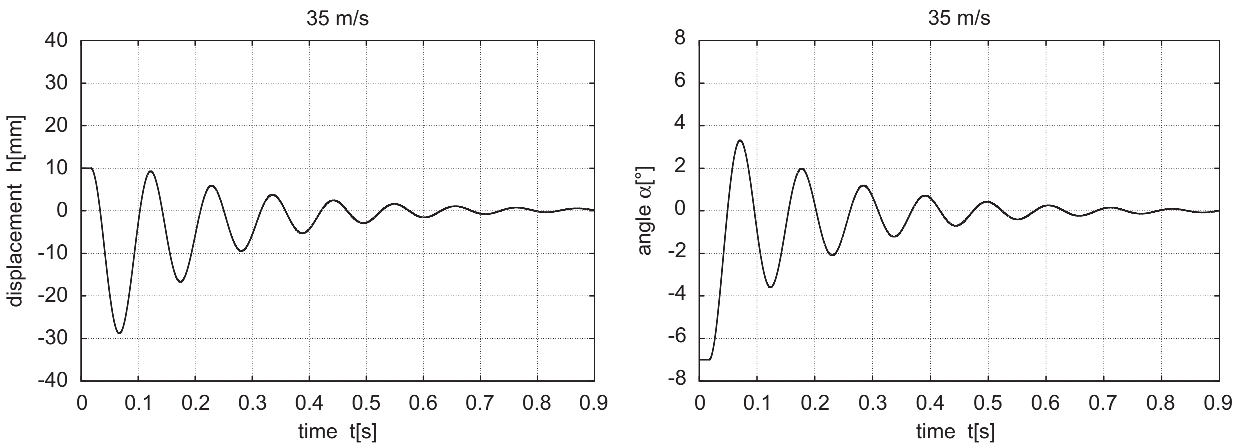

Fig. 3. Flow-induced airfoil vibrations for $U_\infty = 35\,\mathrm{m/s}$.

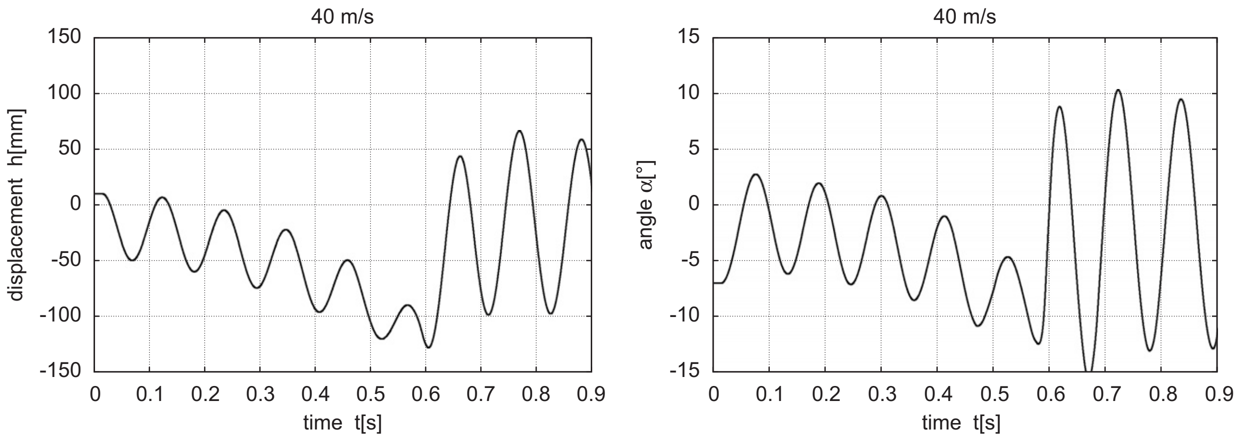

Fig. 4. Flow-induced airfoil vibrations for $U_\infty = 40\,\mathrm{m/s}$.

For far field flow velocity ($U_\infty \leqslant 35\,\mathrm{m/s}$), the displacement H and the rotation angle α are dying in time. When U_∞ exceeds 30 m/s, then the damping of flow-induced vibrations becomes weaker and at about $U_\infty \approx 40\,\mathrm{m/s}$ the system becomes unstable by flutter, the vibrations amplitudes become very high and exceed more than 100 mm and 15° at a limit cycle oscillation (see Fig. 4). Such behaviour of the system is in general agreement with the previous numerical simulations carried out in [15], where no turbulence was considered, but a different airfoil type was modeled.

6. Conclusion

In this paper the numerical method for the simulation of the interaction between viscous incompressible turbulent flow and a vibrating airfoil is developed. The method contains several important ingredients:

- ALE method for the treatment of the time-dependent computational domain,
- time discretization using second-order backward difference formula,
- space discretization by the stabilized finite elements, satisfying the Babuška–Brezzi condition,
- the use of the Reynolds averaged system of equations and the application of algebraic models of turbulence.

The method was applied to the solution of the flow-induced vibrations of the profile NACA 0012. The results prove that the developed method allows the simulation of the interaction of turbulent flow with large Reynolds numbers and the airfoil vibrations with large deformations. The comparison of the described method with the laminar case shows that the turbulent results give more accurate results. For example, in contrast to the turbulent case, in the laminar case, the loss of stability of the system appears at an incorrect lower critical velocity.

The next step in the research will be a further investigation of turbulence models included in the described technique. From the point of view of practical applications, it will be suitable to increase the speed of the computational process by the use of the domain decomposition method and parallelization of the algorithm. A more detailed comparison of the turbulent and laminar flow in the relation to the system behavior is needed.

Acknowledgment

The authors are grateful to Prof. J. Příhoda from the Institute of Thermomechanics of the Academy of Sciences of the Czech Republic in Prague for very valuable and fruitful discussions about turbulence modeling.

References

[1] D. Baldwin, T. Lomax, Thin layer approximation and algebraic model for separated turbulent flows, AIAA Paper (1978) 78–257.
[2] T. Cebeci, A.M.O. Smith, Analysis of Turbulent Boundary Layers, Academic Press, New York, 1974.
[3] T.A. Davis, UMFPACK V4.0. ⟨http://www.cise.ufl.edu/research/sparse/umfpack⟩, University of Florida.
[4] V. Dolejší, ANGENER V3.0. ⟨http://www.karlin.mff.cuni.cz/∼dolejsi/angen/angen.htm⟩, Faculty of Mathematics and Physics, Charles University, Prague.
[5] E.H. Dowell, A Modern Course in Aeroelasticity, Kluwer Academic Publishers, Dodrecht, 1995.
[6] T. Gelhard, G. Lube, M.A. Olshanskii, J.-H. Starcke, Stabilized finite element schemes with LBB-stable elements for incompressible flows, J. Comput. Appl. Math. 177 (2005) 243–267.
[7] P.M. Gresho, R.L. Sani, Incompressible Flow and the Finite Element Method, Wiley, Chichester, 2000.
[8] V. John, Large Eddy Simulation of Turbulent Incompressible Flows, Springer, Berlin, 2004.
[9] G. Lube, Stabilized Galerkin finite element methods for convection dominated and incompressible flow problems, Numerical Analysis and Mathematical Modelling, vol. 29, Banach Center Publications, Warszawa, 1994.
[10] E. Naudasher, D. Rockwell, Flow-Induced Vibrations, A.A. Balkema, Rotterdam, 1994.
[11] T. Nomura, T.J.R. Hughes, An arbitrary Lagrangian–Eulerian finite element method for interaction of fluid and a rigid body, Comput. Methods Appl. Mech. Eng. 95 (1992) 115–138.
[12] P. Rostand, Algebraic turbulence models for the computation of two-dimensional high speed flows using unstructured grids, NASA CR-181741, 1988.
[13] M.M. Stanišić, The Mathematical Theory of Turbulence, Springer, New York, 1988.
[14] P. Sváček, M. Feistauer, Application of a stabilized FEM to problems of aeroelasticity, in: M. Feistauer, V. Dolejší, P. Knobloch, K. Najzar (Eds.), Numerical Mathematics and Advanced Applications, ENUMATH 2003, Springer, Berlin, 2004.
[15] P. Sváček, M. Feistauer, J. Horáček, Numerical simulation of flow induced airfoil vibrations with large amplitudes, J. Fluids Struct. 23 (2007) 391–411.